Monitoring Structural Stability of Trypsin Inhibitor at the Submolecular Level by Amide−Proton Exchange Using Fourier Transform Infrared Spectroscopy: A Test Case for More General Application†

Harmen H. J. de Jongh,‡ Erik Goormaghtigh,* and Jean-Marie Ruysschaert

Laboratoire de Chimie-Physique des Macromolécules aux Interfaces, Université Libre de Bruxelles, CP 206/2, Boulevard du Triomphe, B-1050 Bruxelles, Belgium

Received June 5, 1997; Revised Manuscript Received August 26, 1997⊗

ABSTRACT: Combining the information on the secondary structure content as present in the shape of a protein amide I infrared band with the approach of monitoring amide-proton exchange using infrared spectroscopy, we have been able to investigate the structural stability of different components present in a protein, which are shown to be correlated to the different classes of secondary structures. For this purpose, the changes in intensity in different regions of the amide I have been detected upon exposure of the protein to a ^2H_2O environment, revealing four separate classes of exchanging components. As a test case for the approach described in this work, the amide−proton exchange of hydrated protein films of bovine pancreatic trypsin inhibitor has been studied using infrared spectroscopy, and is compared to literature data obtained by other techniques. A slow amide-proton exchange is observed for a class correlated to the β-strands present in the protein, with protection of amide-protons for more than 19 h. Another class, which has been assigned to mainly helical residues, shows much less protection from exchange. The distribution function of the exchange rates of a class linked to the β-turns displays five times faster exchange rates compared to those found for the majority of the helical residues, but they are still ten times slower compared to a class which we defined to represent the nonstructured parts of the protein.

The advantages of the use of infrared (IR)[1] spectroscopy to obtain structural information on proteins over other biophysical techniques, like X-ray diffraction or nuclear magnetic resonance (NMR), are the relatively small quantities of protein required (50−200 mg) and that it is well applicable to membrane-associated proteins in their lipid environment. The analysis of distinct IR spectral regions can provide us with information on both protein structure and its dynamics. Because the different secondary structures absorb in different regions of the amide I (1700−1600 cm^{-1}), this band has been used for a long time to extract information on the secondary structure content of proteins (Susi et al., 1967; Timasheff et al., 1967). Detection of the changes in intensity in the amide II (1600−1500 cm^{-1}) or amide II′ (1500−1400 cm^{-1}) regions upon exposure of a protein to ^2H_2O, provides information on the tertiary stability of the protein at a molecular level, as these changes have been shown to reflect the exchange of labile amide-protons, whose exchange rates are determined by the structural properties of the protein (Goormaghtigh et al., 1994a; de Jongh et al., 1995). Although one works with protein films when the ATR-IR approach is applied, it has been shown that differences in tertiary stability of a protein are characterized both in films and in aqueous solution by similar differences in amide-proton exchange rates (de Jongh et al., 1995). Recently it was also demonstrated that the apparent pH in protein films spread from buffered aqueous solutions can be retained (de Jongh et al., 1995) and that a similar pH-dependency of the exchange rates has been found for a protein in a film compared to that of the same protein in aqueous solution (Goormaghtigh et al., 1996).

The amide I, primarily arising from C═O stretching (70−85% of the potential energy) together with an out-of-phase CN stretching, a CCN deformation, and a small NH in-plane bending contribution (Krimm & Bandekar, 1986), generally shifts by 5−10 cm^{-1} to lower wavenumber upon exposure of a protein to an ^2H_2O environment [for a review see Goormaghtigh et al. (1994b)]. Detection of these shifts in different regions of amide I should give access to information on the stability of the individual secondary structure types of a protein. In this work we will describe the exchange of the amide-protons of BPTI as the sum of four different classes of exchanging components. The choices made to define these classes are based on the objective to relate them to the different secondary structure types present in the protein. For that reason BPTI was chosen in this study as a test case for this approach, since its structure (Deisenhofer & Steigemann, 1975; Berndt et al., 1992; Schiffer et al., 1994) and amide-proton exchange (Wagner & Wüthrich, 1982; Rashin, 1987; Gallagher et al., 1992; Kim et al., 1993) have been well described in detail by X-ray and NMR techniques. In the accompanying paper (de Jongh et al., 1997) the more general validity and application of this approach is demonstrated by presenting the exchange of

† This work was supported by the Human Capital and Mobility Research Network of the European Commission (Grant No. CHRX-CT92-0018). E.G. is a Senior Research Associate of the National Fund for Scientific Research (Belgium).

* Corresponding author. Tel: +32 2650 5386. FAX: +32 2650 5113.

‡ Present address: Centre for Protein Technology (TNO-WAU), Bomenlaan 2, 6700 EV Wageningen, The Netherlands.

⊗ Abstract published in *Advance ACS Abstracts,* October 15, 1997.

[1] Abbreviations: (ATR) FT-IR, (attenuated total reflection) Fourier transform infrared; BPTI, Bovine pancreatic trypsin inhibitor; TSPA, 3-(trimethylsilyl)-$^2H_4$-propionic acid.

S0006-2960(97)01336-6 CCC: $14.00

several α-, β-, and α-/β-proteins, whose amide-proton exchange is well described in literature, and of those which cannot easily be investigated by NMR techniques, because their size and thus their complexity are too large.

MATERIALS AND METHODS

Protein Purification. Bovine pancreatic trypsin inhibitor (BPTI) was obtained from Sigma (St. Louis, MO). Salts and other low molecular weight components were eliminated by dissolving 20−25 mg of protein in 2.0 mL of 10 mM Tris (pH 6.6, HCl) and elution at 4 °C in 3 mL of 10 mM Tris (pH 6.6, HCl) on a fast desalting column (PD-10 containing 9.1 mL of Sephadex-G25M, Pharmacia), pre-equilibrated with the same buffer. Next the protein was dialyzed four times against 100 times excess triply destilled water at 4 °C. After lyophilization the protein was stored at −20 °C.

A weighed amount of BPTI was dissolved to a final concentration of 10 mg/mL in 10 mM Tris buffer (pH 6.6) containing 25 mM 3-(trimethylsilyl) $^2H_4$-propionic acid (TSPA) (Sigma, St. Louis, MO).

Preparation of Deuterated Proteins. To obtain BPTI in which all labile protons are exchanged for deuterons, 2 mg of protein was dissolved in 150 mL of 10 M urea-d_4 [deuterated as described previously by de Jongh et al. (1992)] in ^2H_2O and incubated for 24 h at room temperature. To remove the urea, the sample was dialyzed 5 times against 34 times excess ^2H_2O at 4 °C, and the protein was subsequently freeze-dried and stored at −20 °C as a stock solution of 10 mg/mL in 10 mM Tris buffer in ^2H_2O (p^{2}H 6.6) containing 25 mM TSPA.

Infrared Measurements. Typically 20 μL of protein stock solution (200 μg) was spread homogeneously on one side of a germanium crystal (50 × 20 × 2 mm, Harrick, Ossining, NY) and dried by a N_2 gas flow. On top of the crystal a 1 mm spacer was placed and the crystal was covered by a stainless steel plate containing a gas in-let and an out-let, allowing the film to become exposed to any controlled atmospheric condition. The crystal was placed under an aperture angle of 45°, yielding 25 internal reflections. Upon exposure of the film to a continuous flow of N_2 gas (30 mL/min), saturated with ^2H_2O by flushing it through four closed 10 mL vials containing 1−2 mL of ^2H_2O each, spectra were recorded every 30 s during the first 10 min and next with exponentially increasing time intervals up to a total of 19 h of exposure, as described previously (de Jongh et al., 1995). All spectra were recorded at room temperature as averages of 16 or 32 scans using a Bruker IFS-55 spectrometer, equipped with a liquid nitrogen cooled mercury cadmium telluride detector in the 0 to 8000 cm^{-1} range with a nominal resolution of 1 cm^{-1}.

Analysis of Infrared Spectra. The digitalization of the spectra was enhanced to 0.5 cm^{-1} by zero-filling of the data prior to Fourier transformation. A full automatic procedure for spectral corrections for atmospheric water contributions and for the integration of various bands in the IR spectra was used, revealing integrals for the amide I, amide II, and amide II′, as described previously (Goormaghtigh et al., 1994a; de Jongh et al., 1995). In this way also the integral of Si−CH_3 band of TSPA (855 ± 10 − 815 ± 10 cm^{-1}) was obtained. All intensities presented are relative to the average intensity in the 1800−1790 cm^{-1} region of the spectra, where no absorption of any of the materials present in the samples is apparent. The relative absorbance is defined as 103 times the detected absorbance, relative to the integral of the TSPA band at 835 cm^{-1}.

RESULTS AND DISCUSSION

Theoretically, the exchange of a labile amide-proton with deuterium for each individual residue in a protein can be studied by detection of the intensity changes at a particular wavenumber within the amide I region caused by the 5−10 cm^{-1} shift to lower wavenumber of its absorption during the time course of exposure of this residue to ^2H_2O (Goormaghtigh et al., 1994c). However, since the dispersion of the individual residues is too low compared to the line width of these absorptions to allow such a detailed analysis and since it is known that the absorptions within the amide I region can be classified according to secondary structure types (Susi et al., 1967; Timasheff et al., 1967), we sustain in this work with the attempt to monitor the exchange behavior of four different classes which could be correlated to the different secondary structure types present in proteins. Two classes are obtained from the information in the 1660−1640 cm^{-1} region, where predominantly the α-helical and nonstructured parts of the protein absorb. A fast (class I) and a slow (class II) exchanging component are discriminated. Another class of exchanging residues is detected by monitoring the spectral intensity at 1620 cm^{-1} (class III), a region where β-stranded residues absorb with little interference from other structure types. A fourth class of exchange is monitored at 1675 cm^{-1} (class IV), where absorptions of both β-turns and β-strands are apparent.

When analyzing intensities in the amide I region we have to take into account three other processes that significantly affect the amide I intensities upon exposure of a protein film to ^2H_2O. These are (1) variations in hydration state of the film, (2) the disappearance of the H_2O contribution from the amide I region, and (3) the different absorptions of the side chains in H_2O and ^2H_2O. First, the magnitude of intensity changes related to these three processes will be investigated and appropriate procedures for correction will be proposed. Next, the exchange of amide-protons of BPTI for four distinct classes will be presented. The results are compared to literature data on the secondary structure and amide-proton exchange of BPTI, and a correlation is derived between these four classes and the secondary structure types. In the accompanying paper we will demonstrate that the procedure as applied in this work on BPTI can also be used to study the structural stability of various other water-soluble globular proteins at a submolecular level.

Effects of the Replacement of H_2O by ^2H_2O in the Amide I Region Not Related to Amide-Proton Exchange

1. Variation in Film Hydration. Upon exposure of a polypeptide film to water-saturated N_2 gas an increased hydration of the film (up to maximally 0.4−0.45 g of water per g of protein) takes place, resulting in an increased film thickness (de Jongh et al., 1996). Since in ATR spectroscopy the absorptivity of the sample decreases exponentially with the distance between the internal reflection element and the film molecules (Harrick, 1967), swelling of a film by increased hydration would decrease its absorptivity. To quantify the changes in intensity due to different degrees of

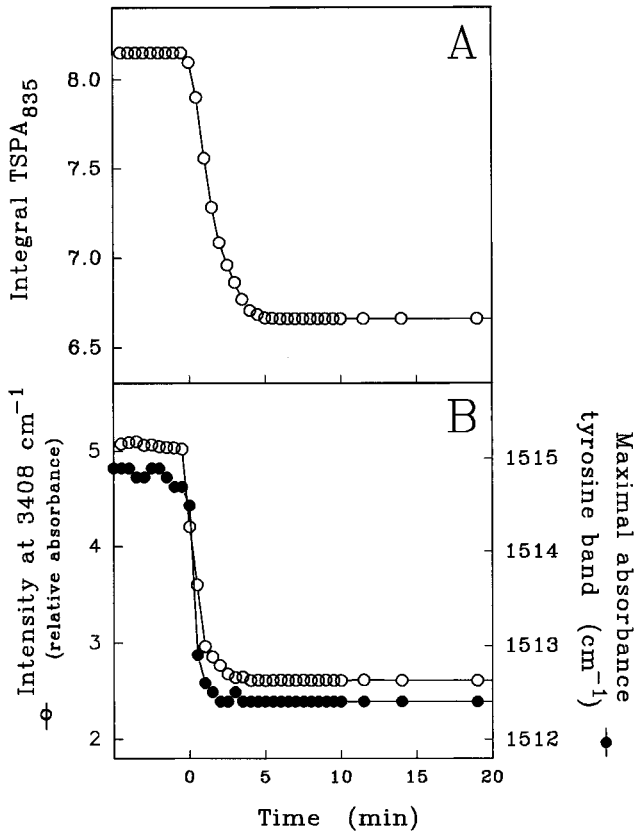

FIGURE 1: (A) Integral of the IR band of 84 mg of TSPA at 835 cm^{-1}, present in a film of 200 mg of BPTI, monitored as a function of time of exposure of the film to ^2H_2O. The integral of this TSPA band is set to an averaged value for the prescans and for those detected from 10 to 1140 min to reduce random fluctuations. (B) IR intensity monitored at 3408 cm^{-1}, representative for the H_2O content of a film of 200 mg of BPTI and 84 mg of TSPA as a function of exposure time (○). The maximum of the IR band of the tyrosine ring absorptions detected in deconvoluted IR spectra is plotted as a function of time of exposure to ^2H_2O (●).

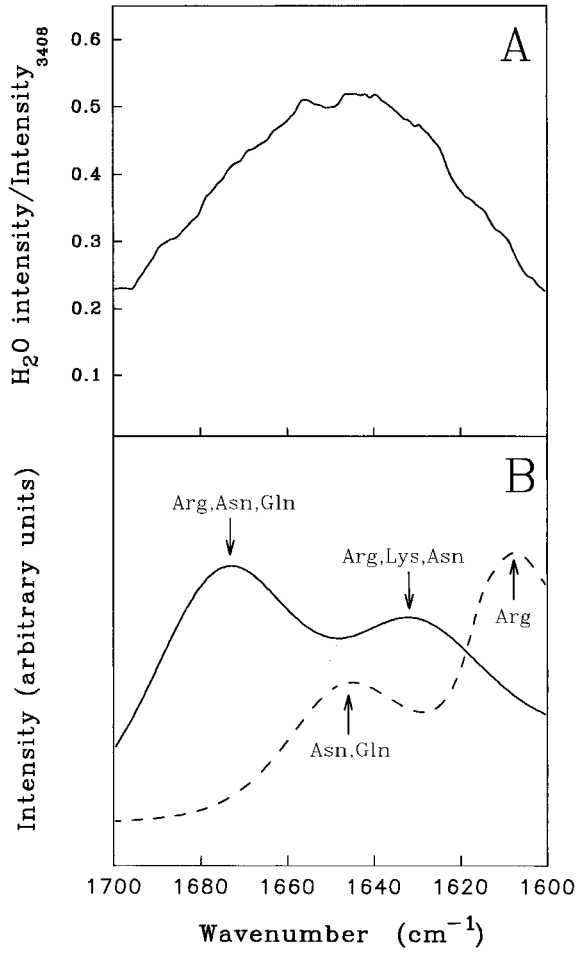

FIGURE 2: (A) Intensity of H_2O at various positions in the amide I region relative to the intensity observed at 3408 cm^{-1}, obtained by comparison of IR spectra of 84 mg of TSPA spread from H_2O compared to that spread from ^2H_2O. (B) Computed IR spectra for the amide I region of the side chain contributions in an H_2O (—) and an ^2H_2O (– –) environment, obtained by summation of the individual contributions according to the amino acid composition of BPTI using the spectral parameters as provided for H_2O by Venyaminov and Kalnin (1991a) and for ^2H_2O by Chirgadze and co-workers (1975). The positions of maximal absorption of the main contributions to the side chain spectrum have been indicated.

hydration, TSPA was chosen as an internal standard for the film because it has an intense Si−CH_3 absorption band around 835 cm^{-1}, distinct from protein bands, and no contribution in the protein amide I region. A more detailed analysis of the use of TSPA as an internal standard for protein films has been described previously (de Jongh et al., 1996). In Figure 1A the integral of the Si−CH_3 band of TSPA, centered at 835 cm^{-1}, is plotted as a function of time of exposure to ^2H_2O-saturated N_2 gas. The decrease of intensity is completed within the first 5 min of the time course and is attributed to swelling of the film. It is straightforward to demonstrate from the wavelength dependency of the absorbance in ATR spectroscopy for films with a thickness much smaller than the wavelength used, as in our cases, that the intensity change due to film swelling occurs in the same proportion at any wavenumber (Harrick, 1967). Amide I intensity variation due to differences in film hydration is therefore accurately compensated for by division of the amide I intensity by the integral of the TSPA band at 835 cm^{-1} for each spectrum recorded during a time course of exchange. Furthermore, possible differences in dielectric constant or refractive index related to a changed hydration state of a protein film, also affecting directly the absorbance of a film (Harrick, 1967), are taken into account.

2. Diminishing H_2O Absorptions in the Amide I Region Due to Replacement by ^2H_2O. Because the protein samples are spread from H_2O solutions, H_2O is still present as hydration water in the films [generally 0.15−0.20 g per g of protein (de Jongh et al., 1996)]. This hydration water has a significant H−O−H bending vibration in the amide I region, whereas the H−O−^{2}H or ^{2}H−O−^{2}H bending vibrations are found outside this spectral region (around 1450 and 1210 cm^{-1}, respectively). Consequently, the replacement of H_2O by ^2H_2O will result in a decrease of intensity in the amide I region. Changes in the H_2O content of a film can be monitored by its stretching vibration band at 3408 cm^{-1} as described previously (de Jongh et al., 1996). At this wavenumber the disappearance of the H_2O absorption can be followed accurately, since the contribution of the relatively weak protein amide A band is negligible. As shown for a BPTI film in Figure 1B the loss of intensity at 3408 cm^{-1} is completed within the first 5 min of exposure of the film to ^2H_2O. Figure 2A reports the intensity of the hydration H_2O contribution in the amide I region, relative to that observed at 3408 cm^{-1}, for a TSPA film in the absence of protein. Assuming that the shape of the hydration H_2O spectrum is similar for protein/TSPA films as for pure TSPA films, one

can correct then the intensities in the amide I region for contributions caused by replacement of H_2O for ^2H_2O by monitoring the intensity change at 3408 cm^{-1} and using the data shown in Figure 2A. In practice, these corrections are maximally 1−2% of the intensity detected in the amide I region.

3. Side Chain Absorptions in H_2O and ^2H_2O. As has been reported, the spectral parameters of side chain absorptions in the amide I region differ significantly in H_2O and ^2H_2O (Chirgadze et al., 1975; Venyaminov & Kalnin, 1991a). Because side chain absorptions might contribute up to 20% of the integrated intensity in the amide I region (de Jongh et al., 1996), it is necessary to correct the intensities in the amide I region for these contributions upon replacement of H_2O by ^2H_2O. Figure 2B shows the calculated side chain spectrum of BPTI in the amide I region for an H_2O and ^2H_2O environment, obtained by superposition of the individual side chain absorptions of the different amino acids present in BPTI using the reported spectral parameters (Chirgadze et al., 1975; Venyaminov & Kalnin, 1991a). Correction for intensity changes in the amide I region caused by the changing environment of the side chains at any wavenumber of interest requires (i) determination of the side chain contribution to the recorded protein spectrum, which is achieved by scaling of the well-resolved tyrosine side chain band at 1515 cm^{-1} of the computed side chain spectrum with that of the recorded protein spectrum, as described in detail previously (de Jongh et al., 1996), (ii) the net difference in absorption of the side chains in H_2O and ^2H_2O environments at the wavenumber of interest, as deduced from the spectra shown in Figure 2B, and (iii) the proportion of deuteration of all individual side chains for every spectrum recorded during the time course. To fulfill also this last requirement, we assume in this work that the fraction of side chains in an H_2O environment parallels the H_2O content of the film as detected at 3408 cm^{-1} (in other words, side chains can only be hydrated with ^2H_2O when H_2O is depleted). Figure 1B justifies this assumption for the case of the tyrosine side chains, as illustrated by the reported shift of the maximum of the tyrosine ring absorption (Chirgadze et al., 1975; Venyaminov & Kalnin, 1991a) from 1514.8 in H_2O to 1512.4 in ^2H_2O (closed circles). For side chains, like those of arginine and glutamic and aspartic acids, it can be stated that generally the exchange of their hydration water is completed within 5 min, based on their intensity shifts in the 1610−1570 cm^{-1} region upon exposure to a ^2H_2O environment (unpublished results on various proteins). Spectral shifts of other side chain absorptions are difficult to detect due to overlap with protein amide bands. In practice, the intensity changes caused by the side chains upon deuteration of the sample contribute generally to 3−5% of the intensity monitored in the amide I.

Measurement of the Exchange Kinetics of Individual Classes. Figure 3 shows the amide I region of four ATR-FTIR spectra of a film of BPTI, at distinct time intervals after initiating amide-proton exchange by exposure of the film to ^2H_2O-saturated N_2 gas. A clear shift of the maximum of the amide I band from 1648 to 1643 cm^{-1} upon exposure to ^2H_2O can be observed. During this time course an increase of intensity in the amide II′ region (1500−1400 cm^{-1}) occurs (not shown), illustrating the exchange of the amide-protons (de Jongh et al., 1995). The corresponding decrease of intensity in the amide II region (1600−1500 cm^{-1}) could not easily be detected (not shown) due to TSPA absorption in this region. Since it was the objective of this work to study the spectral changes taking place in the amide I region, and to correlate them to the various secondary structures present in BPTI, the analyses for the individual exchanging classes are presented here below. To all intensities presented the corrections as described above have been applied.

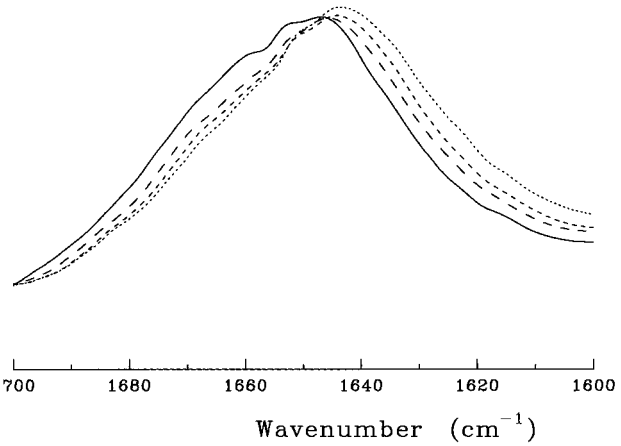

FIGURE 3: IR spectra in the amide I (1800−1700 cm^{-1}) region of a film of 200 mg of BPTI and 84 mg of TSPA, recorded after different time periods of exposure of the film to ^2H_2O-saturated N_2 gas at $t = 0$ (—), $t = 2.5$ min (− −), $t = 11.5$ min (- - -), and $t = 1140$ min (•••). These spectra have only been corrected for atmospheric water contributions by spectral subtraction as described by de Jongh and co-workers (1995). All spectra are relative to the integral of the TSPA band at 835 cm^{-1}.

Class I and Class II Exchange Kinetics. The wavenumbers of maximal absorption of α-helical and random coiled structures are generally close (1658−1652 cm^{-1}) [for a review see Goormaghtigh et al. (1994c)], prohibiting a clear discrimination of the contributions of these two structure types. Any intensity change monitored in this spectral region is a result of the exchange of both the nonstructured and the helical parts. However, when these intensities shift 5−10 cm^{-1} to lower wavenumbers upon exchange, both of these contributions will exhibit an isobestic point in their absorption spectra.

Either successive infrared difference spectra or deconvolution spectra could be used to search for the isobestic point. The advantage of using deconvoluted spectra over difference spectra is that kinetics curve can easily be obtained as shown in Figure 4. Furthermore, the helical component in amide I is expected to be sharper than the disordered component (Chirgadze et al., 1973; Chirgadze & Braznikov, 1974; Venyaminov & Kalnin, 1991b). In turn, the helical component will be rather selectively further narrowed by the deconvolution procedure and thereby will be resolved over the broad disordered. For simplicity we discriminate a fast exchanging component (defined as class I) and a component containing all other exchanging contributions monitored in the 1660−1640 cm^{-1} region (class II). Monitoring the intensity at the isobestic point of one of these two classes will reveal information on the exchange of the other class. Figure 4A shows the same spectra presented in Figure 3, but now after spectral deconvolution using a Lorentzian function with a line width of 40 cm^{-1} followed by a Gaussian apodization function with a 20 cm^{-1} line width [for details see Goormaghtigh and Ruysschaert (1990)]. The isobestic point of the class I is searched by analyzing the first 10 min

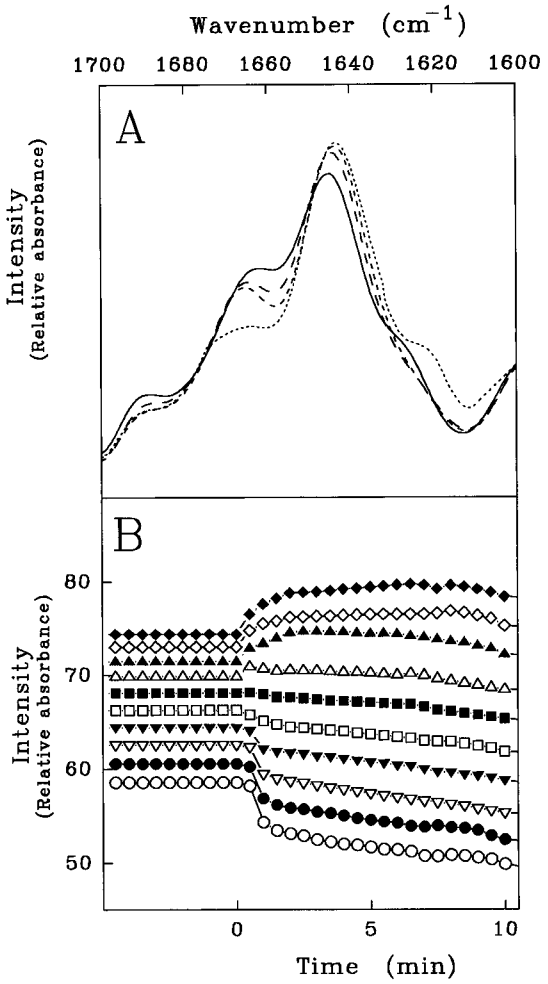

FIGURE 4: (A) The same four IR spectra as shown in Figure 3, but now after deconvolution using a Lorentzian line shape with a line width of 40 cm^{-1}, followed by a Gaussian apodization with a line width of 20 cm^{-1}. (B) The intensity monitored at various positions in the amide I region of IR spectra of a film of 200 mg of BPTI and 84 mg of TSPA, corrected for all contributions related to the replacement of H_2O by ^2H_2O as described in the text, during the prescans and the first 10 min of exposure of the film to ^2H_2O (◆) 1649.5, (◇) 1650, (▲) 1650.5, (▲) 1651, (■) 1651.5, (□) 1652, (▼) 1652.5, (▽) 1653, (●) 1653.5, and (○) 1654 cm)$^{-1}$.

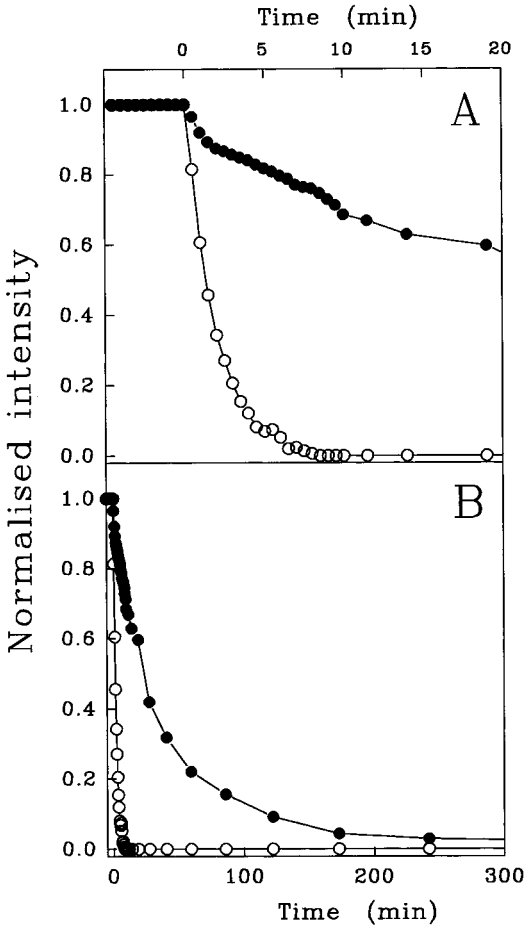

FIGURE 5: Kinetics of exchange of the random coiled (○) and helical (●) structures of BPTI, detected at respectively 1640 and 1652 cm^{-1} in the deconvoluted spectra displayed for the first 20 min only (A) and shown up to 5 h of exposure of the film to ^2H_2O (B). In order to compare class I and class II, we rescaled both kinetics between 1 and 0 with the value of 1 corresponding to the undeuterated samples ($t = 0$).

of the exchange kinetics, as shown in Figure 4B, by evaluation of the intensity of the deconvoluted spectra. Whereas at 1654 cm^{-1} an initial strong decrease in intensity can be observed in the first minute of exchange, at 1649.5 cm^{-1} an increase of intensity is found, indicating that the isobestic point of the class I exchange must be intermediate to these wavenumbers. Since no initial intensity change is observed at 1652 cm^{-1} during the first moments of exposure of the film to ^2H_2O, we define this wavenumber as the isobestic point of the class I exchange. Any intensity change observed at this wavenumber does not belong to the fast exchanging component and is therefore attributed to class II exchange only. It must be stressed here that choosing 1651.5 or 1652.5 cm^{-1} did not significantly affect the results presented in this paper. Interestingly, the slopes of all lines shown in Figure 4B (from 1654 to 1651 cm^{-1}) at longer time of exposure are similar. This suggests that all contributions to the class II exchange detected in this spectral region do have similar spectral features.

Figure 5 shows the kinetics of the class II exchange, monitored at 1652 cm^{-1} in the deconvoluted spectra, upon exposure of the film to ^2H_2O (closed circles). The data have been scaled between 0 and 1 for amide deuteration by making use of data provided by a spectrum of BPTI where all labile protons are replaced by deuterons (see method section). Apparently, the class II amide-proton exchange of BPTI is completed in approximately 4 h (Figure 5B).

In the next section the exchange kinetics for the class I will be determined below (at 1640 cm^{-1}) and above (1656 cm^{-1}) its expected isobestic point by subtraction of the class II contribution. By monitoring the intensity at 1640 cm^{-1} in the deconvoluted spectra during exchange, one detects the increase of intensity of both the random and helical structures (class I + II), since this wavenumber is well below both their expected isobestic points. Knowing the exchange kinetics of class II (as obtained at 1652 cm^{-1}), this contribution can be eliminated from the observed increase of intensity at 1640 cm^{-1} by subtraction. The amplitude of the class II contribution at this wavenumber is obtained by subtraction of the kinetics of this component from the observed intensity at 1640 cm^{-1}, by making the slope of the exchange curve zero between the 14 and 19 h time points. This procedure is based on the assumption that class I exchange does not contain any contribution with a slow exchange behavior. The validity of this choice is discussed later. The result of this subtraction is shown in Figure 5A (open circles), after rescaling between 0 and 100% using the data provided by a

spectrum of BPTI where all labile protons are replaced by deuterons (see Materials and Methods). Obviously, the rate of class I exchange is much faster than that found for the class II contribution of BPTI, and the exchange is completed in approximately 10 min.

It must be stated here that we made the rather arbitrary choice of monitoring the intensity at 1640 cm^{-1}. In fact, we tested various wavenumbers in the 1650−1635 cm^{-1} region and applied for each of these wavenumbers the procedure described above. In all cases similar kinetic observations for the class I component were obtained. However, at wavenumbers lower than 1640 cm^{-1}, interference of the β-stranded contributions could become apparent, whereas at higher wavenumbers the relative contribution of the class II component is larger, making the result of the subtraction procedure less reliable.

To investigate whether the kinetics obtained for the class II component (determined at 1652 cm^{-1}) and that determined for the class I contribution of BPTI (at 1640 cm^{-1}) are sufficient to describe the intensity losses in the 1660−1652 cm^{-1} region of the original spectra shown in Figure 3, we tested whether the decrease of intensity during exchange, for example at 1656 cm^{-1}, a wavenumber higher than the expected isobestic points of the contributions to the class I and class II exchange, could be fitted using the two kinetics obtained (Figure 5). As shown in Figure 6, the observed intensity at 1656 cm^{-1} (open circles) can be fitted by the sum of the two kinetics determined for the class I and class II exchange (dashed line). Alternatively, when the kinetics of exchange of class I is determined by a proportional subtraction of the class II kinetics from the intensity monitored at 1656 cm^{-1}, an exchange curve for class I can be obtained (not shown) that is very similar to that determined using the intensity changes at 1640 cm^{-1} (Figure 5A).

Fitting of the changes in intensity at other wavenumbers in the 1660−1652 cm^{-1} region also revealed good fits, yielding relatively larger class I contributions at higher wavenumbers. The ratios of the class II/class I contributions at 1656 and 1660 cm^{-1} have been determined to be 0.87 and 0.83, respectively. This can be explained by the reported larger line width of random structures compared to that reported for α-helices (Venyaminov & Kalnin, 1991a).

Class III and class IV Exchange Kinetics. While class I and II were defined to account for the nonstructured and α-helical parts of the protein, the class III contribution is supposed to reflect predominantly the exchange of the β-stranded structures present. The increase of intensity during the course of exchange, for example, at 1620 cm^{-1} in the IR spectra (Figure 3) displays the shift to lower wavenumber of pleated β-strands, which, in an H_2O environment, absorb around 1635−1630 cm^{-1} [for a review see Goormaghtigh et al. (1994c)]. At 1620 cm^{-1} the other structure types are expected to have a negligible contribution. A slow exchange is observed for the class III exchange in BPTI (Figure 7A), reaching approximately a 60% exchange after 19 h, based on the intensity at 1620 cm^{-1} for a sample where all labile protons have been exchanged for deuterons (see Materials and Method). When the class III exchange at other wavenumbers in the 1630−1610 cm^{-1} region is monitored, similar exchange curves are found (not shown), with the difference that, at higher wavenumbers, the interference of class I contributions becomes stronger, as reflected by more pronounced initial intensity changes in the first minutes of the time course.

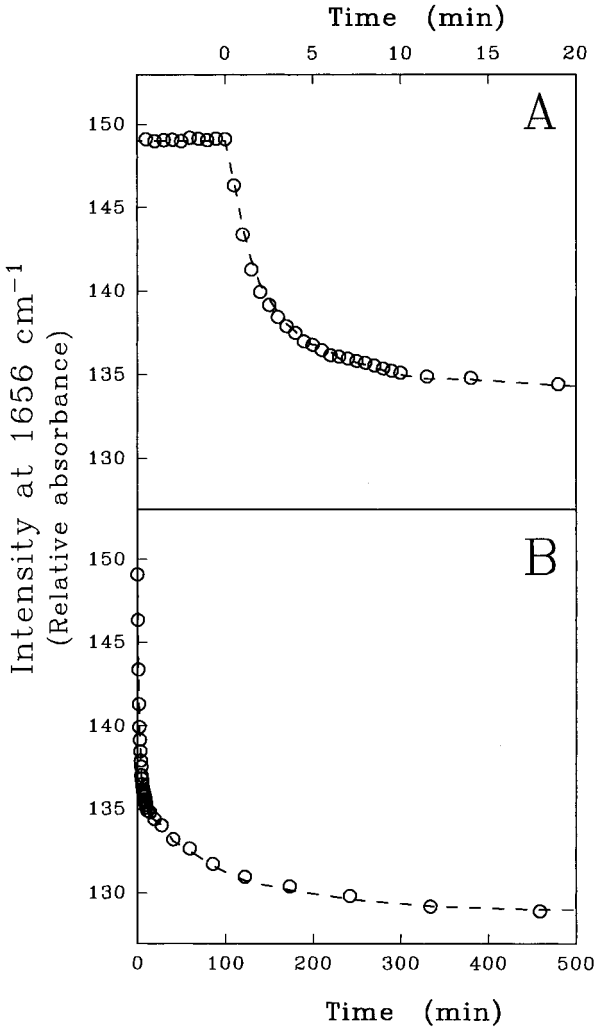

FIGURE 6: Intensity monitored at 1656 cm^{-1} of a film of 200 mg of BPTI and 84 mg of TSPA as a function of time of exposure of the film to ^2H_2O-saturated N_2 gas (open circles). The dashed line represents the summation of the random coiled and the helical contribution as obtained by fitting the data using the two kinetics shown in Figure 5.

β-Turns generally absorb in the 1682−1662 cm^{-1} region [for a review see Goormaghtigh et al. (1994c)]. By monitoring then the IR intensity (Figure 3) at 1675 cm^{-1}, one could detect the shift of this secondary structure type to lower wavenumber upon amide-proton exchange. However, β-strands are also known to have a component of relatively low intensity in the 1689−1682 cm^{-1} region (Goormaghtigh et al., 1994c), which results in an increase of intensity at 1675 cm^{-1} upon exchange. The kinetics of this interfering contribution has been described by the class III exchange, and consequently its contribution to the observed intensity at 1675 cm^{-1} can be eliminated by subtraction, resulting in what is defined as class IV exchange. For this subtraction the assumption is made that at a later stage of the kinetic experiment the slope of the curve is determined by class III amide-proton exchange only. The class IV exchange is shown in Figure 7B, where it can be observed that the class IV contribution to BPTI exchanges within approximately 70 min.

Correlation between Classes of Exchange and Secondary Structure Types. In Table 1 the characteristics of the four

Table 1: Characteristics of the Four Classes of Exchanging Components Contributing to the Intensity Changes Observed in the Amide I Band of BPTI upon Exposure of the Protein Film to ^2H_2O

class	secondary structure element monitored	exchange kinetics monitored at (cm^{-1})	intensity monitored at (cm^{-1})	intensity change (relative absorbance)	percentage secondary structure	
					calculated[a]	reported[b]
I	nonstructured	1640, 1656[c]	1656	10.9	45	48
II	α-helices	1652	1656	9.5	21	19
III	β-strands	1620	1620	13.1	20	22
IV	β-turns	1675[d]	1675	3.0	14	10

[a] Percentages of secondary structure are calculated assuming that only the intended secondary element contributes to the observed class of exchange, using the different relative molar absorptivities (1:0.69:0.33:0.38 for the β-strands:α-helices:β-turns:nonstructured) as reported (de Jongh et al., 1996). [b] Percentages secondary structure as reported in literature determined using NMR and X-ray techniques (Berndt et al., 1992; Schiffer et al., 1994). [c] The class II contribution at this frequency is eliminated by subtraction as explained in the text. [d] The class III contribution at this frequency is eliminated by subtraction as explained in the text.

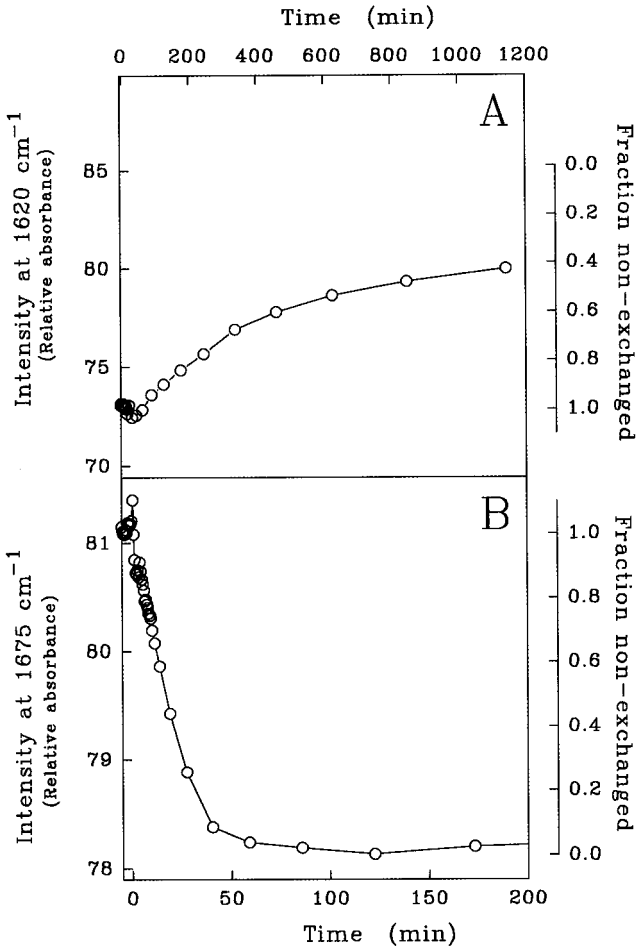

FIGURE 7: (A) The IR intensity monitored at 1620 cm^{-1}, reflecting the exchange of β-strands and (B) at 1675 cm^{-1}, representing the exchange of β-turns, is plotted as a function of the time of exposure of a film of 200 mg of BPTI and 84 mg of TSPA to ^2H_2O. The right axis represents the scale after normalization of the data using the spectrum of a film of BPTI in which all labile protons have been exchanged (see Materials and Methods).

classes of exchange of BPTI are summarized. The difference in the absolute magnitude of the intensity change recorded for each class (before deuteration minus after complete amide-proton exchange) might be correlated to the secondary structure content of BPTI. From the fit shown in Figure 6 it could be deduced that of the total change of intensity at 1656 cm^{-1} is 20.4 units of relative absorbance, the contributions of class I and class II being 9.5 and 10.9 units, respectively. From Figure 7 it can be evaluated that the total intensity changes upon deuteration at 1620 and 1675 cm^{-1} are 13.1 and 3.0 units for class III and class IV, respectively. If these classes represent the individual secondary structures present in BPTI, then these relative contributions should reflect their in the protein. Yet, if a correlation between the intensity changes upon total deuteration for each class and a secondary structure content is to be established, the intensity changes have to be weighted by the molar absorptivities known for each secondary structure. The relative molar absorptivities were shown to be 1:0.69:0.33:0.38 for respectively β-strands:helices:β-turns:random coil (de Jongh et al., 1996). In agreement with usual assignments for the different secondary structure [for a review see Goormaghtigh et al. (1994c)], classes I−IV are expected to correspond to disordered, helical, β-strand, and β-turns structures, respectively. The assumption that the molar absorptivities of the secondary structures are not significantly influenced by deuteration (Chirgadze et al., 1973; Chirgadze & Brazhnikov, 1974; Venyaminov & Kalnin, 1991b) has to be made. After weighting the intensity changes characteristic of every class by the relative molar absorptivities of the corresponding secondary structure, the contribution of the four classes to BPTI are then computed to be 21, 20, 14, and 45%, respectively (Table 1). Remarkably, these numbers correspond closely to the percentages of the reported individual secondary structures of BPTI [19.0, 22.4, 10.3, and 48.3%, respectively (Deisenhofer & Steigemann, 1975; Berndt et al., 1992)], suggesting a clear correlation between the different classes and the secondary structure they are intended to represent.

It must be noted that as far as the very fast exchanging class (class I) is concerned, two effects could modify the amide I band in addition to proton exchange: (1) formation of hydrogen bonds between water molecules and the carbonyl groups of the peptide backbone could produce the shift of the amide I band to lower wavenumber and (2) hydration-induced conformational changes can affect the band shape of the amide I band as revealed for some proteins upon lyophilization (hydration level below 0.04 g of water/g of protein) (Prestrelski et al., 1993). Our measurements could therefore, for class I, represent not only the exchange but also a more general effect due to water accessibility to the protein backbone. Previously we have shown that protein films as prepared here have an average hydration level of 0.15−0.20 g of water per g of protein (de Jongh et al., 1996). Such a degree of hydration was shown to be sufficient to fulfill all hydrogen bonding requirements present in the native protein (Rupley et al., 1980). We therefore expect neither significant changes in hydrogen bonding between water molecules and the peptide backbone nor changes in the conformation of the protein which could affect the shape of

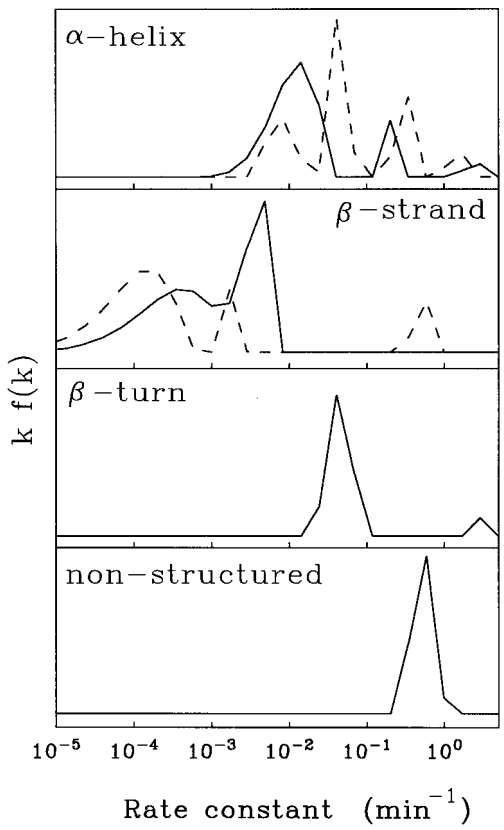

FIGURE 8: Distribution functions of the exchange rates obtained by the IR approach (solid line) and as determined by NMR (dashed line), as presented by Wagner and Wüthrich (1982) for the different (intended) secondary structures present in BPTI, after Laplace transformation of the exchange decay curves.

amide I upon increasing the degree of hydration as might occur during the experiment.

As demonstrated in the accompanying paper, in which we investigate the amide-proton exchange kinetics of eleven other proteins, such a translation to the secondary structure content of a protein is demonstrated to be more generally applicable and the correlation between obtained and reported percentages of secondary structure generally falls within 5% for the different proteins studied.

Exchange Rate Distribution Functions. By subjection of the normalized exchange curves for the different secondary structure types (Figures 5 and 7) to a Laplace transformation, using the algorithm described by Provencher (1982), distribution functions of the exchange rates present in the exchange curves can be obtained, as presented for the four classes of exchanging components as obtained for BPTI in Figure 8 (solid lines). The majority of the class II (α-helical) residues exchange with rates around $10-2$ min^{-1}, with a small fraction of residues exchanging 30 times faster. For the class III (β-stranded) residues slower exchange rates are found, consisting of two populations, centered at 2×10^{-3} and 2×10^{-2} min^{-1}. The class IV (β-turns) has a rather defined exchange rate, approximately 10 times faster than the slow component of the class II residues, whereas the fastest exchange rates are observed for the class I (nonstructured) parts of BPTI.

Comparison with Literature Data on the Amide-Proton Exchange of BPTI. In literature many studies have been presented on amide-proton exchange of BPTI at the level of individual amino acids in aqueous solution (Kim et al., 1993) and in crystals (Gallagher et al., 1992; Kim et al., 1993). The most complete study is that of Wagner and Wüthrich (1982), who determined the exchange rates for each residue at p^{2}H 3.5 and 36 °C in aqueous solution. Previously we have shown that, for reasons which at present are not understood, the exchange in films on germanium crystals is approximately 2−3 times slower compared to that in aqueous solution (de Jongh et al., 1995). Taking this and the difference in the exchange rates between p^{2}H 6.6 and p^{2}H 3.5 into account (Wüthrich & Wagner, 1979), we have extrapolated the kinetics of exchange for the α-helical and β-stranded domains of BPTI to the conditions apparent in this work, using the reported exchange rates (Wagner & Wüthrich, 1982) and secondary structure assignments (Berndt et al., 1992). These exchange curves have subsequently been subjected to a Laplace transformation, and results are presented in Figure 8 (dashed lines). Although the two components observed in the NMR data for the helical component at 10^{-2} and 2×10^{-2} min^{-1} are not resolved in the IR distribution function, the general agreement of the IR and NMR distribution functions is remarkable. The C-terminal helix (residues 3−7) is known to be slightly more stable than the N-terminal one (residues 50−56) (Wagner & Wüthrich, 1982), corresponding to the exchange rate distributions centered at 10^{-2} and 8×10^{-2} min^{-1}. The faster exchange rates (3×10^{-1} min^{-1}) correspond to residues residing at the ends of the helices. A good resemblance between the distribution functions of the IR and NMR data can also be observed for the β-strands. As concluded from the exchange rates found using NMR, the β-strand from residues 29 to 35 is found to be less stable compared to that from residues 18 to 24 (Wagner & Wüthrich, 1982), corresponding with the distribution bands at 8×10^{-3} and 8×10^{-2} min^{-1}, respectively. This biphasic character of the distribution function observed using the IR approach is in full agreement with that observation. That the faster exchanging component (with a rate of 1 min^{-1}) is not observed in the IR data might be explained by a weaker residue H-bonds that consequently have positions at higher wavenumber in the amide I region and are not detected at 1620 cm^{-1}. The good correlation between the literature data and the IR approach described here is a strong indication that the different classes as defined in this work do have a clear correlation to the different secondary structure types, since no mixing of a population of exchanging residues of a particular secondary structure type shows up in the distribution function of another class. The exchange of β-turns and random structured parts is generally poorly defined in NMR data because it often takes place in the "dead time" of the experiment when working at neutral pH.

Comparison of the Exchange Kinetics at the Secondary and Entire Molecule Level. Previously the amide II/I or amide II′/I ratios have been used frequently to detect the amide-proton exchange at the molecular level (Goormaghtigh et al., 1994a; de Jongh et al., 1995; Raussens et al., 1995). Summation of the normalized exchange kinetics of the four individual secondary structures, as shown in Figure 5 for class I and II, and in Figure 7 for class III and IV, multiplied by their proportion of the protein, should then make up the exchange kinetics of the entire protein. In Figure 9 both the normalized exchange obtained by monitoring the amide II′/I region (open circles; experiment not shown) and that obtained by summation of the individual classes (dashed line)

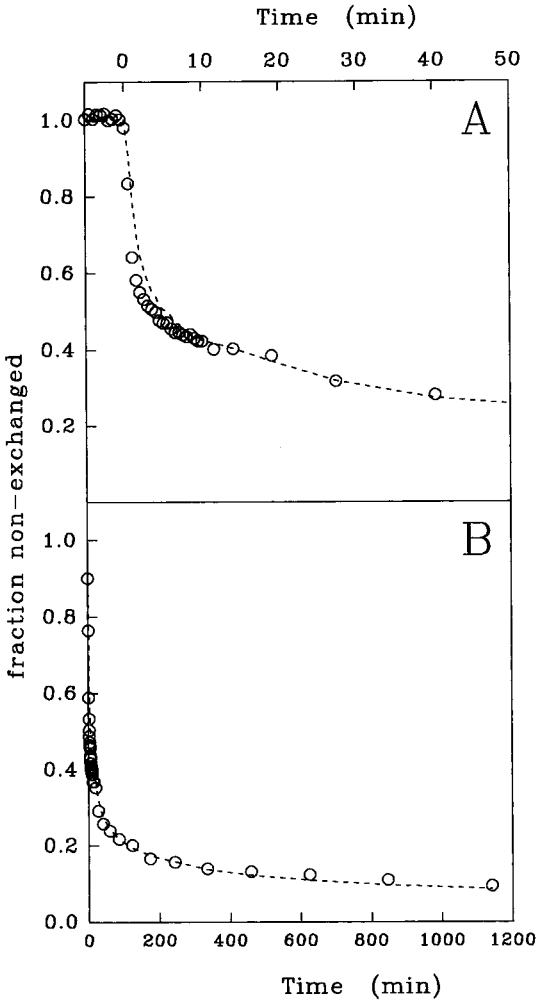

FIGURE 9: Normalized amide II′/amide I ratio plotted as a function of time of exposure of a film of 200 mg of BPTI to ^2H_2O (open circles) (A) during the prescans and the first 50 min and (B) up to 19 h. The dashed line represents the summation of the individual secondary structure contributions to the amide-proton exchange, based on the secondary structure content of the protein and their exchange kinetics as presented in Figures 5 and 7.

are shown. At a longer time scale (Figure 9B) there is a close agreement between these two data sets. However, within the first 10 min of the kinetics some discrepancy appears (Figure 9A), which might be explained by the fact that in the amide II/I ratio no corrections for H_2O or side chain contributions have been made, the intensities of which vary only within those first minutes and lead to a slight overestimation of the amide II/I ratio. The general agreement between the two data sets displayed in Figure 9 indicates that the exchange of all amide-protons of the protein could be detected and described by four classes of amide-protons. The fact that the secondary structure content correlated to the individual classes is in close agreement with the reported structure of BPTI stresses the potentialities of the present approach to record the exchange characteristics of the different secondary structure types.

The presentation of the exchange rate distribution functions and the comparison with reported NMR data (Figure 8), together with the correlation of the sum of the exchange kinetics of the individual structure types with the exchange on the basis of the entire protein (Figure 9), demonstrate the success of the approach described in this work to identify the different exchange rates for the various secondary structure types present in BPTI by monitoring the intensity changes at different wavenumbers within the amide I region of a protein film exposed to ^2H_2O. However, during the procedure to obtain these data we had to make several assumptions, the validity of which will be discussed here subsequently.

To separate both the class II from class I, and the class III from class IV contribution (see Table 1), we assumed that the exchange rates of the class I and class IV were much faster than those of the class II and class III contribution respectively. This assumption has a more general validity since nonstructured parts of proteins do generally have a much faster amide-proton exchange than structured regions (Englander & Kallenbach, 1984; Radford et al., 1992). The success to separate the different classes is demonstrated in Figure 8, since none of the distribution functions presented display similar patterns. However, we can not exclude that, as a consequence of the approach presented here, residues, like those at the helix caps exhibiting almost no structural protection from its amide-proton exchange, would be regarded as being nonstructured. On the other hand, random coiled parts of a protein, having protection from exchange due to tertiary or quartenary structural interactions, might be assigned to be helical in our approach. However, we do expect that the large majority of the helical and nonstructured residues will be classified correctly on the basis of both their position in the amide I region and their exchange behavior. This is demonstrated for eleven other proteins in the accompanying paper (de Jongh et al., 1997).

In theory we could "miss" residues having different positions in the amide I region, like those residing in rippled β-sheets [absorbing around 1640 cm^{-1} (Moore & Krimm, 1976)] or residues having extraordinary hydrogen bonding, for example, to ligands. When the exchange kinetics for a significant number of residues is not accounted for, this will show up by comparison of the summation of the exchange of the individual secondary structures with that of the exchange monitored at a molecular level, like is presented in Figure 9. It should be noted that the correlation between the exchange classes as defined in this work and the secondary structure would be weaker either when the maximal absorption wavenumber of a secondary structure type is significantly different from that assumed in this work or when the molar absorptivity of a particular secondary structure type differs from the average values used here.

Repeating the measurement of amide-proton exchange of BPTI several times revealed that the exchange curves as obtained for the individual secondary structure types deviated within 5% from each other for each time point (data not shown). Although small differences might have already a great impact on the distribution function of the exchange rates, comparable Laplace transforms were obtained, where in all cases similar patterns of fine resolution, indicative for the non-homogeneity within a particular structure type, were observed (data not shown). Also for the analysis of the amide II/I and amide II′/I a similar reproducibility of 5% was found. The estimation of the secondary structure based on the total intensity changes at different regions within the amide I varied by 5−10% for the different experiments (data not shown). As described above, choosing 1660 instead of 1656 cm^{-1} to monitor the class II and class I exchange kinetics affected the ratio between helical and nonstructured contributions less than 5%.

Our approach is shown to be sensitive to non-homogeneous behavior of a secondary structure type (Figure 8), as described for both the helices and the β-strands of BPTI (Wagner & Wüthrich, 1982). This indicates that possible scattering of wavenumbers due to different structural stability does not severely affect the quality of the method of analysis proposed.

Summarizing, in this work we show that the IR approach to study amide-proton exchange at the level of secondary structure of films of BPTI can provide us with quantitative information, which closely correlates to that obtained by NMR techniques. The approach provides also an additional way, besides the present analysis strategies (Goormaghtigh et al., 1990; Surewicz et al., 1993), to obtain information on the secondary structure content of the protein of interest. Although the method is limited to detection at the level of secondary structure, it has no limitations to the complexity of the protein. The more general applicability of this approach will be demonstrated in the accompanying paper, in which the amide-proton exchange of proteins is presented whose structure and dynamics are well characterized by NMR techniques and of those whose complexity prohibits them to be investigated by NMR (de Jongh et al., 1997). We believe that this IR approach might be an additional valuable tool to get insight in the dynamics of proteins at the level of secondary structure, especially when only small quantities of protein are available, or when the particle size is too large, as for membrane proteins.

REFERENCES

Berndt, K. D., Guntert, P., Orbons, L. P., & Wüthrich, K. (1992) *J. Mol. Biol. 227*, 757−775.

Chirgadze, Y. N., & Brazhnikov, E. V. (1974) *Biopolymers 13*, 1701−1712.

Chirgadze, Y. N., Shestopalov, B. V., & Venyaminov, S. Y. (1973) *Biopolymers 12*, 1337−1351.

Chirgadze, Y. N., Fedorov, O. V., & Trushina, N. P. (1975) *Biopolymers 14*, 679−694.

de Jongh, H. H. J., Killian, J. A., & de Kruijff, B. (1992) *Biochemistry 31*, 1636−1643.

de Jongh, H. H. J., Goormaghtigh, E., & Ruysschaert, J.-M. (1995) *Biochemistry 34*, 172−179.

de Jongh, H. H. J., Goormaghtigh, E., & Ruysschaert, J.-M. (1996) *Anal. Biochem. 242*, 95−103.

de Jongh, H. H. J., Goormaghtigh, E., & Ruysschaert, J.-M. (1997) *Biochemistry 36*, 13603−13610.

Deisenhofer, J., & Steigemann, W. (1975) *Acta Crystallogr. B31*, 238−250.

Engl&er, S. W., & Kallenbach, N. R. (1984) *Q. Rev. Biophys*. 16, 521−655.

Gallagher, W., Tao, F., & Woodward, C. K (1992) *Biochemistry 31*, 4673−4680.

Goormaghtigh, E., & Ruysschaert, J.-M. (1990a) in *Molecular description of biological membranes by computer aided conformational analysis* (Brasseur, R., Ed.) Vol. 1, CRC Press Inc., Boca Raton, FL.

Goormaghtigh, E., Cabiaux, V., & Ruysschaert, J.-M. (1990b) *Eur. J. Biochem. 193*, 409−420.

Goormaghtigh, E., Vigneron, L., Scarborough, G., & Ruysschaert, J.-M. (1994a) *J. Biol. Chem. 269*, 27409−27413.

Goormaghtigh, E., Cabiaux, V., & Ruysschaert, J.-M. (1994b) *Subcell. Biochem. 23*, 363−404.

Goormaghtigh, E., Cabiaux, V., & Ruysschaert, J.-M. (1994c) *Subcell. Biochem. 23*, 405−450.

Goormaghtigh, E., de Jongh, H. H. J., & Ruysschaert, J.-M. (1996) *Applied Spectrosc. 50*, 1519−1527.

Harrick, N. J. (1967) in *Internal reflection spectroscopy*, pp 41−66, John Wiley & Sons, New York.

Kim, K.-S., Fuchs, J. A., & Woodward, C. K. (1993) *Biochemistry 32*, 9600−9608.

Krimm, S., & Bandekar, J. (1986) *Adv. Prot. Chem. 38*, 181−364.

Moore, W. H., & Krimm, S. (1976) *Biopolymers 15*, 2439−2464.

Prestrelski, S. J., Tedeshi, N., Arakawa, T., & Carpenter, J. F. (1993) *Biophys. J. 65*, 661−671.

Provencher, S. W. (1982) *Comput. Phys. Commun. 27*, 213−227,−242.

Radford, S. E., Buck, M., Topping, K. D., Dobson, C. M., & Evans, P. A. (1992) *Proteins: Struct., Funct., Genet. 14*, 237−248.

Rashin, A. A. (1987) *J. Mol. Biol. 198*, 339−349.

Raussens, V., Narayanaswami, V., Goormaghtigh, E. Ryan, R. O., & Ruysschaert, J.-M. (1995) *J. Biol. Chem. 270*, 12542−12547.

Rupley, J. A., Yang, P., & Tollin, G. (1980) in *Water in Polymers* (Rowland, S. O., Ed.) pp 111−132, American Chemistry Society, Washington, DC.

Schiffer, C. A., Huber, R., Wüthrich, K., & van Gunsteren, W. F. (1994) *J. Mol. Biol. 241*, 588−599.

Surewicz, W. K., Mantsch, H. H., & Chapman, D. (1993) *Biochemistry 32*, 389−394.

Susi, H., Timasheff, S. N., & Stevens, L. (1967) *J. Biol. Chem. 242*, 5460−5466.

Timasheff, S. N., Susi, H., & Stevens, L. (1967) *J. Biol. Chem. 242*, 5467−5473.

Venyaminov, S. Y., & Kalnin, N. N. (1991a) *Biopolymers 30*, 1243−1257.

Venyaminov, S. Y., & Kalnin, N. N. (1991b) *Biopolymers 30*, 1259−1271.

Wagner, G., & Wüthrich, K. (1982) *J. Mol. Biol. 160*, 343−361.

Wüthrich, K, & Wagner, G. (1979) *J. Mol. Biol. 130*, 1−18.

BI971336X